Spontaneous generation of vortex crystals from forced two-dimensional homogeneous turbulence

Javier Jiménez[a] and Alan Guegan[b]
School of Aeronautics, Universidad Politécnica, 28040 Madrid, Spain

(Received 4 December 2006; accepted 14 June 2007; published online 17 August 2007)

The long-term limit of statistically stationary two-dimensional turbulence is shown to depend on the form of the large-scale forcing, in agreement with previous results. That effect is studied systematically by continuously varying the forcing from deterministic to Brownian in direct numerical simulations in doubly periodic boxes. As expected, this switches on or off the enstrophy cascade and the presence of strong coherent structures, but the transition is not monotonic. Under intermediate forcing conditions, the flow evolves to a stationary vortex crystal with triangular lattice, which appears to be stable and to last indefinitely. Deterministic forcings frustrate crystallization through the formation of fast-moving dipoles, and very random ones melt the crystal. The dispersion properties of the different regimes are studied, and it is shown that efficient particle dispersion depends on the presence of multiscale turbulence. The relation with other two-dimensional systems is discussed. © *2007 American Institute of Physics*.
[DOI: 10.1063/1.2757713]

I. INTRODUCTION

Homogeneous two-dimensional (2D) turbulence is an old but recurring problem in fluid mechanics. The dimensional prediction[1,2] is that the energy should cascade towards larger scales, while the enstrophy, defined as the square of the root-mean-square (rms) vorticity ω', cascades to smaller ones with an exponent $\alpha=3$ for the energy spectrum $E(k) \sim k^{-\alpha}$. It was soon realized that the eddy turnover time $(k^3E)^{-1/2}$ is independent of the eddy size when $\alpha=3$, so that enstrophy transfer cannot be local in wavenumber.[3] A consequence is that the enstrophy cascade is not expected to be universal and depends on the forcing.[4,5] This is contrary to the three-dimensional (3D) case, where $\alpha=5/3$ for the direct energy cascade and the characteristic time decreases as $k^{-2/3}$ for the high wavenumbers. The cascade is then spectrally local and the small eddies quickly become independent of the forcing. In fact, most 2D numerical simulations fail to reproduce the dimensional theory, particularly for the direct cascade. Decaying flows have spectra steeper than predicted, which can be traced to the appearance of stable coherent vortices that dominate the flow[6–8] and shelter the enstrophy from cascading.[9] In statistically stationary forced turbulence, the flow separates into coherent and interstitial vorticity, and the latter behaves as an almost passive scalar under the effect of the vortices.[10–12] Ideally, the interstitial component should emerge from the shadow of the vortices at very large Reynolds numbers,[11] but this has only been observed with time-uncorrelated forcings that explicitly destroy the large-scale structures.[13–15] Slightly more complicated forcings result in $\alpha \approx 3$, but with nonuniversal prefactors.[16]

[a]Also at: Center for Turbulence Research, Stanford University. Electronic mail: jimenez@torroja.dmt.upm.es
[b]Present address: LadHyX, École Polytechnique, Palaiseau, France.

II. NUMERICAL EXPERIMENTS

To study systematically the effect of the forcing scheme we use two-dimensional direct numerical simulations in spatially 2π-periodic boxes. We use a standard vorticity-stream function Fourier code, dealiased by the two-thirds rule, with third-order Runge-Kutta time advancement. The vorticity satisfies

$$\mathrm{D}_t\omega = (-1)^n \nu \nabla^{2n} \omega + F, \tag{1}$$

where D_t is the Lagrangian derivative. It is driven to statistical equilibrium by the forcing F, which acts on the wavevector shell $k_1 \leqslant k = |\mathbf{k}| \leqslant k_2$. In addition, the flow is subject in $k \leqslant k_0$ to a linear friction, $-\mu\omega$, which damps the energy carried in that direction by the inverse cascade. In this paper, $k_1=5$, $k_2=10$, and $k_0=3$.

The forcing combines two schemes whose enstrophy injection rates per unit mass, η_r and η_d, are kept fixed for each simulation. The first is a Brownian torque,

$$F^r_{\mathbf{k}} = (\eta_r/2N_f\Delta t)^{1/2}\mathcal{R}, \tag{2}$$

where N_f is the total number of modes being forced, Δt is the numerical time step, and the real and imaginary parts of $\mathcal{R}$ are random numbers uniformly distributed in the interval $\pm\sqrt{3}$, with zero mean and unit variance, independently chosen for each numerical time step and for each Fourier mode.

The second scheme is a linear amplification, similar to the negative viscosity often used in three-dimensional simulations,[17]

$$F^d_{\mathbf{k}} = (\eta_d/2Z_f)\hat{\omega}_{\mathbf{k}}, \tag{3}$$

where $\hat{\omega}_{\mathbf{k}}$ is the coefficient of $\exp(\mathrm{i}\mathbf{k}\cdot\mathbf{x})$ in the Fourier expansion of ω, and Z_f is the instantaneous total enstrophy contained within the forcing band, defined as the integral of the instantaneous vorticity spectrum over the appropriate

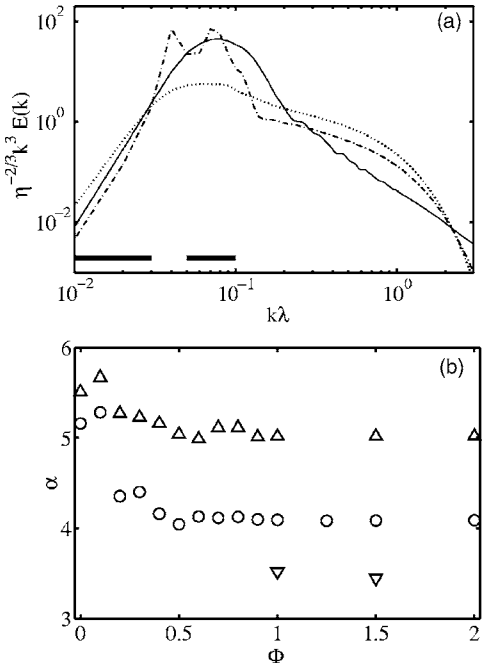

FIG. 1. (a) Enstrophy spectral density, $k^3E(k)$, in viscous units. $n=1$, Re=7000. $\Phi=0$ (—); (----) 0.5; (···) 1.0. The two horizontal segments are the ranges for forcing and for low-wavenumber damping. (b) Slope of the energy spectrum. (△) $n=1$, Re=1400; (○) $n=1$, Re=7000; (▽) $n=4$, Re=12 500.

wavenumbers. This type of forcing may model, for example, some large-scale instability.

At equilibrium, the sum of the "random" and "deterministic" enstrophy inputs, $\eta=\eta_r+\eta_d$, equals the mean total enstrophy dissipation rate. The primary forcing parameter is the fraction of the enstrophy input due to the random torque, $\Phi=\eta_r/\eta$. We will see below that the deterministic amplification promotes the formation of large coherent vortices, and we will present some results using $\Phi>1$. This will allow us to go "beyond" purely random forcing by damping the coherent enstrophy in the forcing band. The damped enstrophy is compensated by an increase of the the random torque, and, because Brownian forcing changes rapidly with time, it is quickly advected outside the forcing band by the nonuniform background flow.

The low-wavenumber damping was fixed to $\mu=0.1\,\eta^{1/3}$ after some experimentation. This ensured a statistically stationary energy and an enstrophy spectral peak located within the forcing band [Fig. 1(a)]. It was verified *a posteriori* that the enstrophy dissipated by this friction is a negligible fraction of the total, so that η can be safely used as a surrogate for the viscous enstrophy dissipation. It is important to realize at this point that, because of the spatial periodicity of the velocities, the total circulation in the computational box is always zero. Forcing introduces enstrophy, but no circulation.

There is a natural Reynolds number $\mathrm{Re}=\nu^{-1/n}L^2\eta^{1/3n}$, based on the injection wavelength $L=4\pi/(k_1+k_2)$, and, assuming a k^{-3} spectrum, a viscous dissipation scale λ such that $L/\lambda=\mathrm{Re}^{1/2}$. Most of our simulations use regular viscosity $n=1$, Re=7000, and 1024^2 collocation points. Some were repeated for comparison at $n=4$ hyperviscosity and Re=12 500, and at $n=1$, Re=1400, and 512^2 resolution. The effects described below are always observed, becoming more pronounced at the higher Reynolds numbers. Note, however, that, since the main conclusion of this paper will be that the final state of forced two-dimensional turbulence depends on the forcing method, there is no guarantee that the same results would have been obtained with a different pair of forcing schemes.

Compensated spectra for three representative cases are given in Fig. 1(a). Spectral slopes, obtained over the part of each spectrum that looks visually like a power law, are shown in Fig. 1(b). The two higher Φ have a short $\alpha\approx4$ power-law range, which corresponds to the interstitial vorticity. This slope decreases from $\alpha\approx5$ to 3.4 from the low-Reynolds-number to the hyperviscous cases. Previous randomly forced simulations[11] suggest that it would tend to the theoretical $\alpha=3$ at very high Re. The lowest values of Φ are dominated by a strong peak at $kL\approx4$, which implies coherent structures of that size that do not participate in the cascade. When $\Phi\leqslant0.2$, the interstitial spectrum is absent. The steeper spectral exponents of those cases, $\alpha=5-6$, are typical of fields with few vortices,[8] and are probably associated with the approximately discontinuous vorticity at the vortex edges, caused by mutual stripping of their outer layers,[18] and observable in individual fields. True discontinuities[19] would yield $\alpha=4$. Note that when $\alpha>5$, or when the large-scale peak is strong enough, the spectral density of viscous enstrophy dissipation, $k^5E(k)$, peaks at large scales, and the enstrophy is dissipated directly in the coherent structures. For such flows the enstrophy cascade and λ are irrelevant. Only for $\Phi>0.5$ does small-scale viscous dissipation become dominant in the present cases.

The evolution of the flow is slow, especially for the deterministically forced cases, and the simulations ran for times of the order of $\omega' t\approx6000$ after reaching statistical equilibrium. Some deterministic hyperviscous cases were run almost ten times longer, and even then, failed to reach statistical equilibrium. Although they coalesced into individual vortices relatively early, their enstrophy continued to increase linearly during the simulation at a rate very close to the injection rate η.

In fact, since we have seen that the dissipation happens in those cases at the injection scale, L, their evolution time is the viscous one, $t_v\approx L^{2n}/\nu$, and, equating the dissipation to the injection rate, the equilibrium enstrophy is given by $\nu\omega'^2\approx\eta L^{2n}$. It then follows that $\omega' t_v\approx\mathrm{Re}^{3n/2}$, which becomes impractically long at high Reynolds numbers. In our hyperviscous cases, this estimate suggests evolution times of the order of $\omega' t=10^9$.

III. THE VORTICAL STRUCTURES

Structures of sizes comparable to the injection wavelength appear in all cases, but, whereas deterministic forcings tend to stabilize a few vortices on a weak background, random ones continually inject background vorticity that deforms into smaller vortices and filaments (Fig. 2). In fact, it is easy to see that, even when the random forcing is only

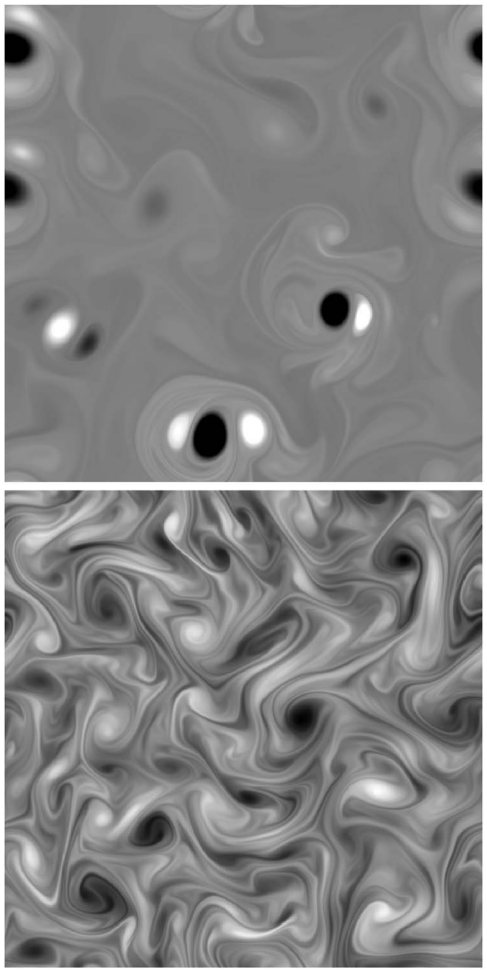

FIG. 2. Vorticity. (Top) $\Phi=0$. (Bottom) $\Phi=1.5$. The grayscale spans in both cases the range $\pm 4\omega'$. $n=1$, Re=7000.

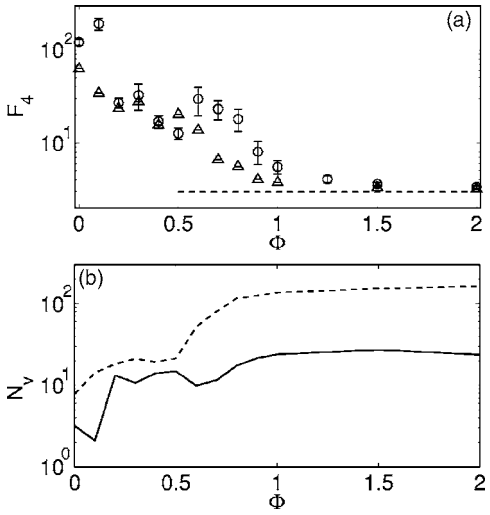

FIG. 3. (a) Fourth-order flatness of the vorticity as a function of Φ. (----) Gaussian. Error bars are one σ. $n=1$. (△) Re=1400; (○) Re=7000. (b) Number of coherent vortices. (—) $D>L/2$; (----) all vortices. $n=1$, Re=7000.

applied at a single wavenumber, advection by the nonuniform velocity field aliases it to become effectively broadband. Figure 3(a) shows that this is reflected in the vorticity probability density functions, which have strong tails and high flatness for small Φ, but become roughly Gaussian above $\Phi\approx 1$. Note that, as mentioned in the previous section, the effect is present for the two Reynolds numbers represented in Fig. 3(a), and that it is more pronounced for the higher Re. The same will be seen below in Figs. 5(b) and 6.

Coherent vortices are arbitrarily defined as contiguous objects whose vorticity magnitude is larger than ω', and over which the mean vorticity discriminant[20] is negative. Their diameters are defined from their areas S as $S=\pi D^2/4$, and their number is plotted as a function of Φ in Fig. 3(b), with large vortices with $D>L/2$ plotted separately. For $\Phi\lesssim 0.2$ the flow is dominated by the few dipoles and tripoles seen in Fig. 2(a). For $\Phi\gtrsim 0.2$ there is a population of coherent vortices whose sizes are roughly half of the injection wavelength. Their number is roughly equal to 15 below $\Phi\approx 0.6$, and grows only weakly, to about 20, for higher Φ. The total number of vortices is also low for small Φ, but it increases sharply to $N_v\approx 200$ above $\Phi\approx 0.5$. Those smaller vortices have a wide distribution of sizes and are presumably implicated in the enstrophy cascade. The fraction of the total enstrophy contained in the coherent vortices decreases from 0.95 at $\Phi=0$ to 0.8 at $\Phi\approx 0.7$, and vortex characteristics stay approximately constant above that value. These numbers are roughly independent of Re, although the number of small-scale vortices increases considerably with Re and with hyperviscosity.

It is interesting that, even if the coherent forcing tends to create and maintain large vortices, their number and intensity stay roughly constant in time. This is achieved by a gradual growth of the enstrophy as the structures intensify, followed by occasional annihilations of a vortex pair in which the enstrophy suddenly decreases by 5%–10%. The average period between those events depends on Φ, but it is of the order of $\omega' t\approx 300$–1000. Even for $\Phi=0$, the annihilations represents less than 10% of the total time-averaged enstrophy dissipation.

IV. VORTEX CRYSTALS

The most interesting cases are $\Phi=0.3$–0.6, which relax to form stable vortex crystals at all the Reynolds numbers and hyperviscosities investigated, becoming clearer for the higher Re. An example is shown in Fig. 4. All the crystals show the triangular lattice in that figure and, as mentioned above, the number of large vortices is always close to 16. This is presumably related to the forcing wavenumber. In an infinite triangular lattice, N_v vortices form $2N_v$ triangles, whose unit area is therefore $2\pi^2/N_v$. This implies in our case that the side of each triangle is approximately $2L$, which is of the order of either the wider edge of the forcing band, or of the narrower edge of the low-wavenumber damping.

Although the total circulation is zero, all the coherent vortices are of the same sign, with the opposite vorticity having been shredded into the interstitial fluid. This is not due to an asymmetry in the code. In most simulations, the ratio between the total area of the positive and negative coherent vortices is very close to unity. Of the 11 cases in

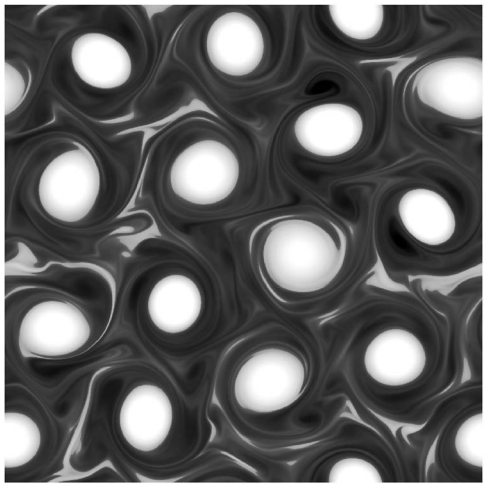

FIG. 4. Vorticity for $\Phi=0.5$. The coherent vortices are, in this case, positive. Other parameters as in Fig. 2.

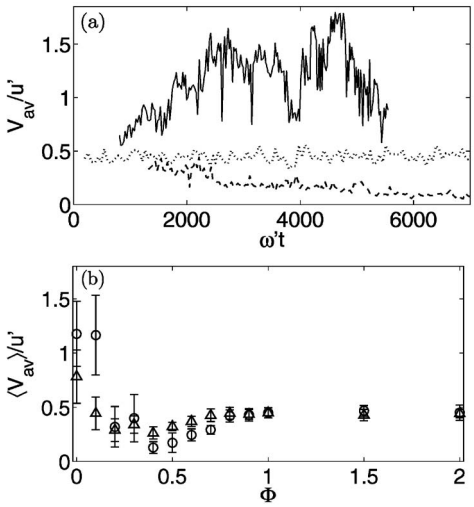

FIG. 5. (a) Temporal evolution of the vortex mobility. $n=1$, Re=7000. $\Phi=0$ (—); (----) 0.5; (·····) 1.0. (b) Mean vortex mobility vs Φ. $n=1$. (△) Re=1400; (○) Re=7000.

which it is not, which correspond to those that can be classified as crystals, positive vortices predominate in 6 of them, and negative ones in the other 5.

Lattices of point vortices have been investigated in detail,[21] and the triangular is the only stable simple lattice in a doubly periodic domain.[22] No stable infinite lattices of two-signed vortices are known. This probably explains why our simulations tend to be singly signed, since the flow would spontaneously evolve away from unstable configurations and into the stable ones.

To quantify the degree of crystallization we compute the vortex mobility, defined by selecting the 12 largest vortices in each flow field, and computing for each of them the magnitude of the average of the flow velocity, taken over all the points interior to the vortex. The mobility is the area-weighted mean,

$$V_{av}=\sum_j \left|\int_{S_j} u\mathrm{d}^2\mathbf{x}\right| \Big/ \sum_j \int_{S_j} \mathrm{d}^2\mathbf{x}, \tag{4}$$

of these magnitudes. Its temporal evolution is given in Fig. 5(a) for three cases. Its temporal average and standard deviation, taken over the last 30% of each simulation, are given in Fig. 5(b) as a function of Φ. They are normalized with the rms flow velocity magnitude u'. The analysis was repeated with the largest 20, instead of 12, vortices, with basically identical results. It is clear from the figures that the identification of large vortices is essentially unambiguous.

The high vortex mobilities of the two lowest Φ are seen visually to be due to the dipoles that dominate them. Because they have very low net circulation, they interact weakly and travel in essentially straight lines until they bump into another vortex, which they typically disrupt. A moderate amount of random forcing is apparently enough to destroy them, and the flow crystallizes naturally, as in the case $\Phi=0.5$ in Fig. 5(a). The cases with $\Phi=0.2$ and $\Phi=0.3$ took longer to crystallize, but they eventually reached a state very similar to that in Fig. 4. For $\Phi\geqslant 0.6$ the disorder introduced by the forcing progressively disrupts the crystal, and very little order is left above $\Phi=0.8$.

An interesting consequence of the different flow configurations that result from the forcing schemes is that the diffusion characteristics also change. Figure 6 shows the dispersion coefficient of single massless particles as a function of Φ, obtained by fitting their mean-square displacement $\langle|\mathbf{x}-\mathbf{x}_0|^2\rangle$ to $2Dt$. This method can only describe approximately the dispersion in the deterministic cases, in which the particles circle for long times around individual vortices. These orbits have periods of the order of $2\pi L/u'$, which in our case is $\omega' T\approx 30$, and amplitudes of order L. Every 10–20 orbits, on average, the particle flies to a neighboring vortex, a distance $O(2L)$ away, where it is trapped again. The dispersion observed in our simulations, over times $\omega' t\approx 3000$, corresponds therefore to 5–10 flights, which is probably too short for describing it as a regular diffusion phenomenon. Nevertheless, the result of a discrete Brownian motion of amplitude $\pm 2L$, every $\omega' t\approx 400$, corresponds reasonably well with the coefficients, $D\omega'/u'^2\approx 0.2$, given for the crystals in Fig. 6.

The dispersion coefficients for the random cases are of the order as those reported in Ref. 23 for forced two-dimensional turbulence in the inverse-cascade regime, $D\omega'/u'^2\approx 6$. The difference between the two cases, a factor of about 2, is reasonable considering that the two flows are in

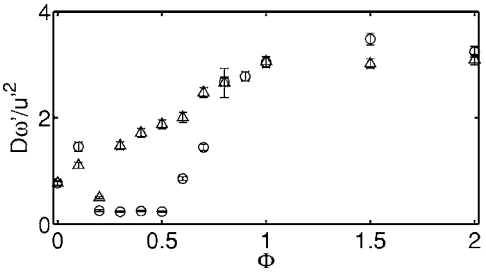

FIG. 6. One-particle diffusion coefficient. $n=1$. (△) Re=1400; (○) Re=7000.

a different cascade regime and do not even have similar energy spectra.

Vortex crystals have previously been observed in the decay of two-dimensional turbulence in highly magnetized electron plasmas in circular containers, both experimentally[24] and numerically,[25] in rotating superfluids[26] and in Bose-Einstein condensates (BEC).[27] In those cases all the vortices have one sign, and the pattern rotates, although configurations with a central vortex of the opposite sign and zero total circulation have been shown to be stable.[28,29] Extended triangular lattices have been observed in BEC[30] and, in a slightly different context, in superconductors in a magnetic field.[31,32] They represent local minima of the system energy,[21] and it has been argued that the initial presence of background incoherent vorticity in plasmas provides the "friction" required to drive the system to that state.[33] In what may be a related phenomenon, the inverse cascade in two-dimensional turbulence, forced at small scales in a periodic box, eventually condenses into what can be considered as a vortex crystal in which the unit cell is the computational box itself.[34]

To our knowledge the flows reported here are the first in which such states are achieved naturally in forced noncircular geometries with vorticity of both signs. The new crystals are stationary configurations, and it is tempting to interpret the required random forcing as playing the same function as the interstitial vorticity of the decay experiments, although we have mentioned that its immediate effect is to prevent the formation of stable dipoles. In an observation reminiscent of the present results, it was hypothesized in Ref. 27 that crystals in BEC should only be observed for an intermediate range of temperatures. Since the two-dimensional vorticity equation (1) is invariant to the addition of an arbitrary solid-body rotation, at least in the absence of forcing, the present stationary states can be related to rotating ones by subtracting a uniform vorticity. In that sense, their vortices are also singly signed.

V. DISCUSSION AND CONCLUSIONS

In summary we have shown that, in agreement with previous evidence, stationary two-dimensional turbulence depends on the nature of the forcing, with the enstrophy cascade switching on or off according to the amount of forcing randomness. The transition is, however, not monotonic. For mostly deterministic forcings, the flow develops a few coherent structures that, at least for the present conditions, coalesce into a gas of dipoles or tripoles that survive for long times moving at high speeds. When the forcing is random, the dipoles are broken and weaker coherent structures coexist with interstitial randomized vorticity whose spectrum appears to approach the theoretical k^{-3} limit as the Reynolds numbers increases. Only for these randomly forced cases does the enstrophy dissipate predominantly at high wavenumbers. When strong coherent structures are present, viscous dissipation occurs in them. Under forcings with an intermediate amount of randomness the flow relaxes into vortex crystals that are stable and appear to last indefinitely. For those steady-state flows the direct enstrophy cascade is absent, and forcing and dissipation happens in the same wavenumber range. The pitch of the crystal lattice is therefore determined by the forcing wavenumber, but its symmetry is selected by the flow nonlinearity. In all our experiments the lattice turned out to be triangular, which is the only known stable state for lattices of point vortices. Not much is known about the stability of lattices of vortex patches, but the analysis of a somewhat similar problem regarding the stability of a Kármán street of vortex patches[35] showed that systems of inviscid patches retain the stability properties of the corresponding systems of point vortices if they are symmetric enough.

We have also noted that similar crystal states are found experimentally in other two-dimensional physical systems, although to our knowledge this is the first case in which the system has been found to respond directly to forcing.

It is unclear whether such states are of more than academic interest, but it may be mentioned that the slow diffusion in the stationary crystals might be useful in reducing the transport properties of highly magnetized plasmas, which behave largely as two-dimensional fluids.[24]

ACKNOWLEDGMENTS

This work was supported in part by the CICYT, under Contract No. TRA2006-08226, and by the TMR EU network (No. HPRN-CT-2002-00300).

[1] R. H. Kraichnan, "Inertial ranges in two-dimensional turbulence," Phys. Fluids **10**, 1417 (1967).
[2] G. K. Batchelor, "Computation of the energy spectrum in homogeneous two dimensional turbulence," Phys. Fluids **12**, 233 (1969).
[3] R. H. Kraichnan, "Inertial range transfer in two- and three-dimensional turbulence," J. Fluid Mech. **47**, 525 (1971).
[4] M. E. Maltrud and G. K. Vallis, "Energy spectra and coherent structures in forced two-dimensional and beta-plane turbulence," J. Fluid Mech. **228**, 321 (1991).
[5] J. R. Herring and J. C. McWilliams, "Comparison of direct numerical simulation of two-dimensional closure with two-point closure: the effect of intermittency," J. Fluid Mech. **153**, 229 (1985).
[6] B. Fornberg, "A numerical study of 2-D turbulence," J. Comput. Phys. **25**, 1 (1977).
[7] J. C. McWilliams, "The emergence of isolated coherent vortices in turbulent flow," J. Fluid Mech. **146**, 21 (1984).
[8] R. Benzi, G. Paladin, S. Patarnello, P. Santangelo, and A. Vulpiani, "Intermittency and coherent structures in two-dimensional turbulence," J. Phys. A **19**, 3771 (1986).
[9] J. C. McWilliams, "A demonstration of the suppression of turbulent cascades by coherent vortices in two-dimensional turbulence," Phys. Fluids A **2**, 547 (1990).
[10] B. Legras, P. Santangelo, and R. Benzi, "High resolution numerical experiments for forced two-dimensional turbulence," Europhys. Lett. **5**, 37 (1988).
[11] K. Ohkitani, "Wave number space dynamics of enstrophy cascade in a forced two-dimensional turbulence," Phys. Fluids A **3**, 1598 (1991).
[12] K. G. Oetzel and G. K. Vallis, "Strain, vortices and the enstrophy inertial range in two-dimensional turbulence," Phys. Fluids **9**, 2991 (1997).
[13] V. Borue, "Spectral exponents of enstrophy cascade in stationary two-dimensional homogeneous turbulence," Phys. Rev. Lett. **71**, 3967 (1993).
[14] T. Gotoh, "Energy spectrum in the inertial and dissipation ranges of two-dimensional steady turbulence," Phys. Rev. E **57**, 2984 (1998).
[15] C. Pasquero and G. Falkovich, "Stationary spectrum of vorticity cascade in two-dimensional turbulence," Phys. Rev. E **65**, 056305 (2002).
[16] Y. Kaneda and T. Ishihara, "Nonuniversal k^{-3} energy spectrum in stationary two-dimensional homogeneous turbulence," Phys. Fluids **13**, 1431 (2001).
[17] R. S. Rogallo, "Numerical experiments in homogeneous turbulence,"

NASA Technical Memo No. 81315, 1981. Available at http://ntrs.nasa.gov/
[18]B. Legras, D. G. Dritschel, and P. Caillol, "The erosion of a distributed two-dimensional vortex in a background straining flow," J. Fluid Mech. **441**, 369 (2001).
[19]P. G. Saffman, "On the spectrum and decay of random two-dimensional vorticity distributions at large Reynolds number," Stud. Appl. Math. **50**, 377 (1971).
[20]J. Weiss, "The dynamics of enstrophy transfer in two-dimensional hydrodynamics," Physica D **48**, 273 (1991).
[21]H. Aref, "Vortex crystals," Mar. Technol. Soc. J. **39**, 1 (2002).
[22]V. K. Tkachenko, "Stability of vortex lattices," Sov. Phys. JETP **23**, 1049 (1966).
[23]C. Pasquero, A. Provenzale, and A. Babiano, "Parameterization of dispersion in two-dimensional turbulence," J. Fluid Mech. **439**, 279 (2001).
[24]K. S. Fine, A. C. Cass, W. G. Flynn, and C. F. Driscoll, "Relaxation of 2D turbulence to vortex crystals," Phys. Rev. Lett. **75**, 3277 (1995).
[25]D. A. Schecter, D. H. E. Dubin, K. S. Fine, and C. F. Driscoll, "Vortex crystals from 2D Euler flow: Experiment and simulation," Phys. Fluids **11**, 905 (1999).
[26]E. J. Yarmchuk and M. J. V. Gordon, "Observation of stationary vortex arrays in rotating superfluid Helium," Phys. Rev. Lett. **43**, 214 (1979).
[27]K. W. Madison, V. Bretin, and J. Dalibard, "Stationary states of a rotating Bose-Einstein condensate: Routes to vortex nucleation," Phys. Rev. Lett. **86**, 4443 (2001).
[28]R. M. Schoemaker, H. J. H. Clercx, and G. J. F. van Heist, "Stability and transport properties of multiple-patch quasiequilibria," Phys. Fluids **16**, 3656 (2004).
[29]D. G. Crowdy, "Exact solutions for rotating vortex arrays with finite-area cores," J. Fluid Mech. **409**, 209 (2002).
[30]J. R. Abo-Shaeer, C. Raman, J. M. Vogels, and W. Ketterle, "Observation of vortex lattices in Bose-Einstein condensates," Science **292**, 476 (2001).
[31]A. A. Abrikosov, "On the magnetic properties of superconductors of the second group," Sov. Phys. JETP **5**, 1174 (1957).
[32]U. Essmann and H. Träuble, "The direct observation of individual flux lines in type II superconductors," Phys. Lett. **24A**, 526 (1967).
[33]D. Z. Jin and D. H. E. Dubin, "Theory of vortex crystal formation in two-dimensional turbulence," Phys. Plasmas **7**, 1719 (2000).
[34]L. M. Smith and V. Yakhot, "Bose condensation and small-scale structure generation in a random-force driven 2D turbulence," Phys. Rev. Lett. **71**, 352 (1993).
[35]J. Jiménez, "On the linear stability of the inviscid Kármán vortex street," J. Fluid Mech. **178**, 177 (1987).